



REMOVAL OF METHYLENE BLUE FROM WATER USING ACID-ACTIVATED BENTONITE CLAY: A FEASIBILITY STUDY

REMOÇÃO DE AZUL DE METILENO DA ÁGUA UTILIZANDO ARGILA BENTONITA ATIVADA COM ÁCIDO: UM ESTUDO DE VIABILIDADE

ELIMINACIÓN DE AZUL DE METILENO DEL AGUA UTILIZANDO ARCILLA BENTONITA ACTIVADA CON ÁCIDO: UN ESTUDIO DE VIABILIDAD

Lucas Santos Almeida

Graduated in Materials Engineering
Institution: Universidade Federal Rural do Rio de Janeiro
Address: Rio de Janeiro, Rio de Janeiro, Brazil
E-mail: luccass.a@hotmail.com

Renata Nunes Oliveira

PhD in Metallurgy and Materials Science Institution: Universidade Federal Rural do Rio de Janeiro Address: Rio de Janeiro, Rio de Janeiro, Brazil E-mail: renatanunes.ufrrj@gmail.com

Belmira Benedita de Lima Kuhn

PhD in Metallurgy and Materials Science Institution: Universidade Federal Rural do Rio de Janeiro Address: Rio de Janeiro, Rio de Janeiro, Brazil E-mail: belmira@ufrrj.br

Tessie Gouvea da Cruz Lopes

PhD in Engineering Institution: Universidade Federal Rural do Rio de Janeiro Address: Rio de Janeiro, Rio de Janeiro, Brazil E-mail: tessie@ufrrj.br

Antonieta Middea

PhD in Polymer Science and Engineering Institution: Centro de Tecnologia Mineral (CETEM) Address: Rio de Janeiro, Rio de Janeiro, Brazil E-mail: amiddea@cetem.gov.br

Edla Maria Bezerra Lima

Master's in Engineering Geology and Environmental Geology Institution: Empresa Brasileira de Pesquisa Agropecuária - Embrapa Tecnologia de Alimentos

Address: Campinas, São Paulo, Brazil E-mail: edla.lima@embrapa.br





Antonio Renato Bigansolli

PhD in Materials Science Institution: Universidade Federal Rural do Rio de Janeiro Address: Rio de Janeiro, Rio de Janeiro, Brazil E-mail: bigansolli@ufrrj.br

ABSTRACT

This study highlights the significance of acid functionalization in enhancing the adsorption capacity of bentonite clay from Novo Hamburgo, Brazil, for the efficient removal of methylene blue (MB) from wastewater. Employing hydrochloric (HCl) or sulfuric acid (H₂SO₄) for acid activation, we demonstrate a substantial improvement in the clay's surface properties and adsorption efficiency. A comprehensive characterization using X-ray diffraction (XRD), Fourier-transform infrared spectroscopy (FTIR), scanning electron microscopy with energy dispersive spectroscopy (SEM/EDS), and ImageJ software analysis revealed distinct effects of acid treatments. Notably, HCl treatment preserved essential components like Al₂O₃ and Fe₂O₃, whereas H₂SO₄ resulted in significant leaching. The acid-activated samples exhibited remarkable methylene blue adsorption, confirmed by UV-VIS spectroscopy. The enhanced adsorption capacity of acid-activated bentonite clay compared to natural clay underscores its potential as a costeffective and efficient adsorbent for cationic dye removal. These findings contribute to sustainable wastewater treatment solutions, emphasizing the importance of acid functionalization and the reliability of UV-VIS spectroscopy for monitoring adsorption processes. The study demonstrates the potential of acid-activated bentonite clay for practical applications in wastewater treatment.

Keywords: acid-activated bentonite clay, acid treatment, adsorption, methylene blue removal, acid functionalization.

RESUMO

Este estudo destaca a importância da funcionalização ácida no aumento da capacidade de adsorção da argila bentonita de Novo Hamburgo, Brasil, para a remoção eficiente do azul de metileno (MB) de águas residuais. Utilizando ácido clorídrico (HCl) ou ácido sulfúrico (H₂SO₄) para ativação ácida, demonstramos uma melhoria substancial nas propriedades de superfície e eficiência de adsorção da argila. Uma caracterização abrangente utilizando difração de raios X (XRD), espectroscopia de infravermelho com transformada de Fourier (FTIR), microscopia eletrônica de varredura com espectroscopia de energia dispersiva (SEM/EDS) e análise de software ImageJ revelou efeitos distintos dos tratamentos ácidos. Notavelmente, o tratamento com HCl preservou componentes essenciais como Al₂O₃ e Fe₂O₃, enquanto o H₂SO₄ resultou em lixiviação significativa. As amostras ativadas com ácido exibiram adsorção notável de azul de metileno, confirmada por espectroscopia UV-VIS. A capacidade de adsorção aumentada da argila bentonita ativada com ácido em comparação com a argila natural destaca seu potencial como um adsorvente eficaz e econômico para a remoção de corantes catiônicos. Essas descobertas contribuem para soluções sustentáveis de tratamento de águas residuais, enfatizando a importância da funcionalização ácida e a confiabilidade da espectroscopia UV-VIS para monitorar processos de adsorção. O estudo demonstra o potencial da argila bentonita ativada com





ácido para aplicações práticas no tratamento de águas residuais.

Palavras-chave: bentonita ativada com ácido, tratamento ácido, adsorção, remoção de azul de metileno, funcionalização ácida.

RESUMEN

Este estudio destaca la importancia de la funcionalización ácida en el aumento de la capacidad de adsorción de la arcilla bentonita de Novo Hamburgo, Brasil, para la eliminación eficiente del azul de metileno (MB) de aguas residuales. Empleando ácido clorhídrico (HCl) o ácido sulfúrico (H2SO₄) para la activación ácida, demostramos una mejora sustancial en las propiedades de superficie y eficiencia de adsorción de la arcilla. Una caracterización exhaustiva utilizando difracción de rayos X (XRD), espectroscopía infrarroja con transformada de Fourier (FTIR), microscopía electrónica de barrido con espectroscopía de energía dispersiva (SEM/EDS) y análisis de software ImageJ reveló efectos distintos de los tratamientos ácidos. Notablemente, el tratamiento con HCl preservó componentes esenciales como Al₂O₃ y Fe₂O₃, mientras que el H₂SO₄ resultó en una lixiviación significativa. Las muestras activadas con ácido exhibieron una adsorción notable de azul de metileno, confirmada por espectroscopía UV-VIS. La capacidad de adsorción mejorada de la arcilla bentonita activada con ácido en comparación con la arcilla natural subraya su potencial como adsorbente eficaz y económico para la eliminación de tintes catiónicos. Estos hallazgos contribuyen a soluciones sostenibles de tratamiento de aguas residuales, enfatizando la importancia de la funcionalización ácida y la confiabilidad de la espectroscopía UV-VIS para monitorear procesos de adsorción. El estudio demuestra el potencial de la arcilla bentonita activada con ácido para aplicaciones prácticas en el tratamiento de aguas residuales.

Palabras clave: arcilla bentonita activada con ácido, tratamiento ácido, adsorción, eliminación de azul de metileno, funcionalización ácida.

1 INTRODUCTION

Methylene Blue (MB) is a cationic dye with the molecular formula $C_{16}H_{18}ClN_3S$ and a molar mass of 319.85 g/mol, known for its high water solubility and intense blue color. Its molecular structure features a positively charged cationic group, which confers a strong affinity for negatively charged surfaces, enabling efficient adsorption onto diverse materials. The release of MB-laden wastewater into natural water bodies poses a significant threat to aquatic life and ecosystems, with potentially devastating consequences. Moreover, the human health implications of MB-contaminated wastewater are alarming, as it is a known toxicant that harms aquatic organisms, including fish, algae,





and invertebrates, by disrupting respiratory and metabolic processes, thereby jeopardizing the delicate balance of aquatic ecosystems (Dehghani *et al.*, 2017; Dimbo *et al.*, 2024). Adsorption has proven to be a viable and efficient method for eliminating MB from wastewater by attaching MB molecules to the surface of solid adsorbents.

Bentonite, a versatile and widely available solid adsorbent, boasts extensive global reserves, with key reserve holders including Brazil, China, the United States, Turkey, Greece, and India. In Brazil, bentonite deposits are predominantly located in São Paulo (33.6%), Paraíba (49.8%), and Bahia (15.3%), with the latter two situated in the country's northeast region. Due to their large reserves, low cost, and limited adsorptive and catalytic properties, bentonites are often subjected to chemical activation using inorganic acids to enhance their surface properties. This process increases the surface area, surface acidity, pore size, and thermal stability of bentonite, rendering it suitable for applications as catalysts, catalytic supports, adsorbents, and more (Caglar *et al.*, 2013; Ullah *et al.*, 2016; Gandhi *et al.*, 2022; Borah *et al.*, 2022).

Bentonite clays belong to the smectite group, characterized by a 2:1 layered structure consisting of two tetrahedral sheets and one octahedral sheet. The smectite group exhibits a high cation exchange capacity (CEC) ranging from 70 to 150 meq/100g, which is influenced by the size and charge of ions in solution. Cations with high valence and low hydration tend to have higher exchange capacities. The CEC is also affected by the degree of hydration, with larger ions exhibiting lower hydration degrees and higher selectivities (Díaz and Santos, 2001; Santos *et al.*, 2015; Bangar *et al.*, 2023).

Smectites, including bentonite, can be classified as sodic or calcium, depending on the dominant exchangeable cation (Na⁺ or Ca²⁺) and their capacity for mineral expansion through water absorption. The high specific surface area of smectites directly influences their physicochemical and technological properties, making them suitable for various applications, including: Oil industry (thixotropic fluids in well drilling); paint and varnish industry (thickeners); civil construction (waterproofing for dams and landfills) and adsorbents (heavy metals and pigments) (Aishat *et al.*, 2015; Soares *et al.*, 2017; Chaari *et al.*, 2019).

Several researchers have highlighted the importance of acid activation of bentonites for producing catalysts and adsorbents. Calcium bentonites are often treated





with HCl or H₂SO₄ acid, as the cation exchange is related to the size and hydration power of ions. The acid activation process can significantly enhance the surface properties of bentonite, making it a valuable material for various industrial applications (Díaz and Santos, 2001; Su *et al.*, 2014; Chaari *et al.*, 2019; Hamad *et al.*, 2024).

Studies have shown that acid treatment of bentonite clay can significantly impact its surface area and adsorption capacity (Leodopoulos *et al.*, 2015; Belkhir *et al.*, 2024). As could be seen in a Nigerian bentonite clay treated with 2M HCl or 2M H₂SO₄ demonstrated adsorption capacity for heavy metals, with H₂SO₄ treatment yielding higher adsorption capacity (Nwosu *et al.*, 2018; Abdullahi *et al.*, 2020).

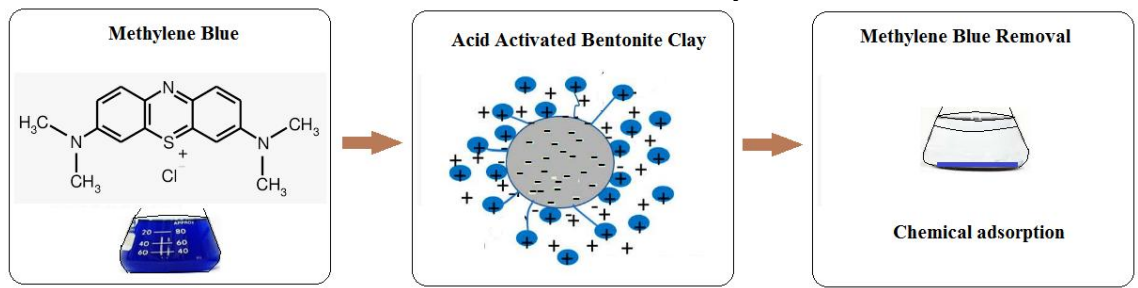
However, excessive acid treatment can lead to a decrease in surface area and adsorption capacity. For instance, a Dijah-Monkin bentonite clay treated with 3M HCl solution for 3.5h showed a 27% reduction in surface area and decreased MB adsorption (Alexander *et al.*, 2018). The acid activation process can alter the cation exchange capacity and surface properties of bentonite, affecting its adsorption mechanisms. Two mechanisms are responsible for MB+ adsorption: cation exchange and reversible physical adsorption. Acid activation can leach out exchangeable cations, decreasing the activity of the first mechanism and the overall adsorption capacity (Alexander *et al.*, 2012). A significant knowledge gap exists in the acid treatment of raw bentonite, a crucial aspect of optimizing its adsorption properties. Recent studies have underscored this gap, with few investigations exploring this topic (Rigo *et al.*, 2006; Couto Junior *et al.*, 2013; Fajardo *et al.*, 2017; Lima *et al.*, 2019).

To address this void, our research focuses on the acid activation of a bentonite clay from Novo Hamburgo, Brazil, using HCl or H₂SO₄. By investigating the adsorption process (control monitored by UV-Vis spectroscopy), this study aims to evaluate the effectiveness of acid-treated bentonite in removing methylene blue (MB) from aqueous solutions, thereby contributing to the development of efficient wastewater treatment technologies. Schematic procedure shown in the Figure 1.





Figure 1. Scheme illustrating the removal process of methylene blue from aqueous solution by adsorption onto acid-activated bentonite clay.



Source: Prepared by the authors themselves.

2 EXPERIMENTAL

Bentonite clay (Na-35, designated as 'raw bentonite') was provided by Schumacher Insumos. The received clay particles had a size inferior to 0.074 mm (200 mesh). Acid activation was carried out on 1g of bentonite clay using 100 mL of 6 M sulfuric acid (VETEC) or 100 mL of 6 M hydrochloric acid (VETEC) at 90°C for 0.5h or 1h, under magnetic stirring (EVEN). Samples treated with hydrochloric acid were labeled NA-C, while those treated with sulfuric acid were labeled NA-S. Following acid activation, the samples were cooled to room temperature and washed with distilled water until a pH of 5-6 was reached. The samples were then oven-dried at 50°C for 36h and manually disaggregated using an agate mortar.

X-ray diffraction (XRD) analysis of the samples (raw bentonite clay and acid-treated bentonite clays) was performed using a Rigaku Miniflex II Desktop diffractometer with Cu-K α radiation, operating in the 2 θ range of 10-90° at a scan rate of 0.05°/s. The spectra were evaluated using the Powder Diffraction Database PDF-2 and the Diffrac.EVA software (Centre for Mineral Technology-CETEM). The degree of crystallinity (χ c) of the samples was calculated according to Eq 1, where A is the area of the curve and Aa is the amorphous area. The amorphous area (Aa) was estimated by fitting a Gaussian curve to the diffractograms of the raw bentonite, HCl-1h, and H₂SO₄-1h samples using the OriginPro software.





$$\chi c = 100((A-Aa))/A$$
 (1)

The samples were further characterized by Fourier Transform Infrared (FTIR) spectroscopy using a VERTEX 70 spectrometer in Attenuated Total Reflectance (ATR) mode with a PLATINUM ATR accessory. The spectra were collected over a range of 4000 to 400 cm⁻¹ with 32 scans per sample.

Backscattered electron images were obtained using a LEO 1450 VP scanning electron microscope (SEM) coupled with an energy dispersive spectroscop (EDS) detector. The SEM images were analyzed using the public domain software ImageJ. To distinguish particles from the background, the images of the raw and acid-treated clays were segmented using the threshold tool. The "Analyze Particles" plugin was then used to calculate particle size (Feret's diameter) and shape (circularity) parameters."

The adsorption potential of the samples was evaluated using a UV-VIS spectrophotometer (KASUAKI equipment). The adsorption test involved mixing 1g of bentonite clay (activated or non-activated) with 10 mL of 2 mM aqueous methylene blue (MB) solution, performed in triplicate for 6h. All samples were analyzed at a wavelength of 400 nm. A standard curve for MB was constructed using solutions of 1 mM, 2 mM, and 3 mM, evaluated at the same wavelength. The results were statistically analyzed using two-way ANOVA (95% confidence level), with 'type of acid' (HCl and H₂SO₄) and 'activation time' (0h, 0.5h, and 1h) as factors, followed by a Tukey test (95% confidence level). This preliminary adsorption study provides valuable insights into the adsorption behavior of the bentonite clay samples, paving the way for future improvements and optimizations.

3 RESULTS AND DISCUSSIONS

3.1 RAW BENTONITE CLAY (NA-35)

The SEM/EDS backscattered electron (BSE) image of raw bentonite clay (Figure 2a) revealed a platelet shape and relatively homogeneous morphology (González-Santamaria *et al.*, 2021). The corresponding elemental analysis (Figure 2b) showed a high





content of SiO₂ (60.2%), followed by Al₂O₃ (20.9%) and Fe₂O₃ (9.1%), as expected. Additionally, smaller amounts of Na₂O (4.7%), MgO (3.7%), and CaO (1.4%) were detected (Moraes *et al.*, 2010; Mano *et al.*, 2014). Notably, Brazilian clays exhibit varied compositions depending on the region of origin due to their sedimentary nature and widespread presence throughout the country (Moraes *et al.*, 2010). Furthermore, these clays typically possess exchangeable cations (Na⁺, Mg²⁺, Ca²⁺) due to their negatively charged layers (De León *et al.*, 2003; Carmo *et al.*, 2021).

Figure 2c presents the X-ray diffraction (XRD) results. The diffractogram exhibits peaks with decreased intensity, which are summarized in Table 1 (experimental 2θ values). The theoretical patterns of the matched phases are also listed in Table 1, including the corresponding Powder Diffraction File (PDF) entries from the PDF-2 database and the associated (hkl) planes. The raw bentonite (Na-35) was found to contain montmorillonite (MMT), quartz (Q), mica (M), albite (A), and halloysite (H) (Ulakpa *et al.*, 2022).

Additionally, Fourier Transform Infrared (FTIR) spectroscopy revealed characteristic bands associated with aluminosilicate materials, as shown in Figure 2d and detailed also in Table 1 (Moraes *et al.*, 2010; Zhirong *et al.*, 2011; Bonilla-Blancas *et al.*, 2019; Pimraksa *et al.*, 2020).





Figure 2. (a) SEM/BSE image; (b) semi-quantitative elemental composition (wt%) obtained by SEM/EDS; (c) X-ray diffraction (XRD) pattern; and (d) Fourier Transform Infrared (FTIR) spectrum of raw bentonite clay (Na-35).

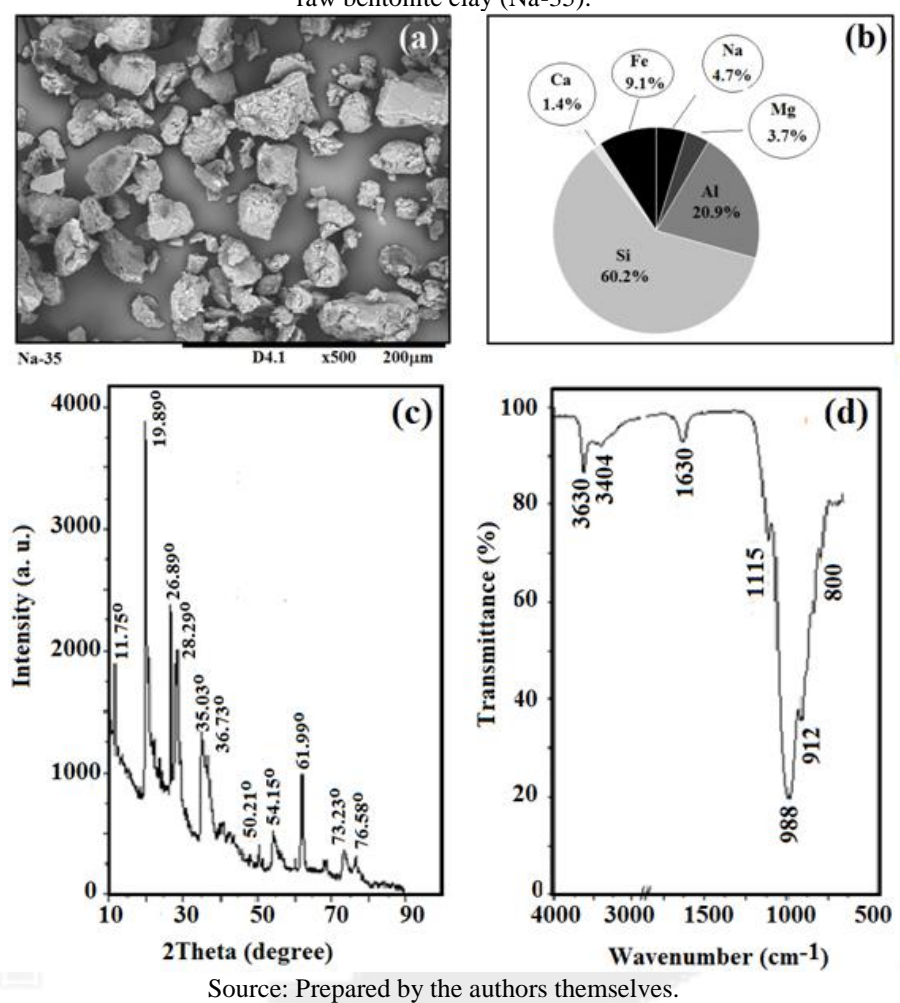


Table 1. FTIR and XRD analysis of the raw bentonite (Na-35), with the following phase identifications: MMT (montmorillonite), Q (quartz), F (feldspar), A (albite), H (hydrotalcite), and NI (not identified).

1711711 (1	with (monthornomic), & (quartz), i (leidspar), ii (mydrotaleite), and it (not identified).						
FTIR			XRD				
Bands	Vibration mode (Moraes	2θ (°)	File (PDF2)	2θ (°)	(hkl)		
(cm ⁻¹)	et al., 2010; Zhirong et	exp.		theor.			
	al., 2011; Bonilla-						
	Blancas et al., 2019;						
	Pimraksa <i>et al.</i> , 2020)						
3630	v(structural OH groups)	19.92	MMT (03-0015)	19.89	NI		
3404	hydroxyls bound via	26.76	MMT (03-0015); Q (65-	26.83;	NI; (101)		
	hydrogen bonds		0466)	26.63			
1630	H-O-H in water	28.44	A (71-1150)	28.55	(220)		
1115	silicate groups	27.94	F (89-8574); A (71-1150)	27.84;	(002); (040);		
				27.80	$(\overline{2}02)$		
988	Si-O-(Si or Al)	28.20	A (71-1150); F (89-8574)	28.09;	(002); (220)		
	, ,		,,,,,,,,,,,,,,,,,,,,,,,,,,,,,,,,,,,,,,,	28.12	, ,, ,		
912	Al-Al-OH	20.90	Q (65-0466)	20.85	(100)		
800	quartz admixture to	11.74	H (02-0229)	11.82	NI		
	1		` '				



bentonite				
	35.12	MMT (03-0015)	35.30	NI
	22.14	F (89-8574); A (71-1150)	22.05;	$(\overline{2}01); (\overline{2}01)$
			22.00	,,,,,,
	62.04	MMT (03-0015); H (02-	61.79;	NI; NI
		0229)	62.26	
	36.68	Q (65-0466)	36.54	(110)
	23.78	F (89-8574)	23.89	(130)
	23.54	A (71-1150)	23.71	$(111)(\overline{1}30)$
	24.48	A (71-1150)	24.47	$(131)(\overline{13}0)$
	40.80	Q (65-0466)	39.46	(012)
	54.14	MMT (03-0015); H (02-	54.23;	NI; NI
		0229)	53.88	
	73.44	MMT (03-0015); H (02-	73.33;	NI; NI
		0229)	73.33	
	76.54	H (02-0229)	76.80	NI
	50.24	Q (65-0466)	50.13	(112)
	68.44	Q (65-0466)	68.13	(023)

*theor. = theoretical; exp.=experimental. Source: Prepared by the authors themselves.

3.2 ACID TREATED BENTONITE – HCL (NA-C)

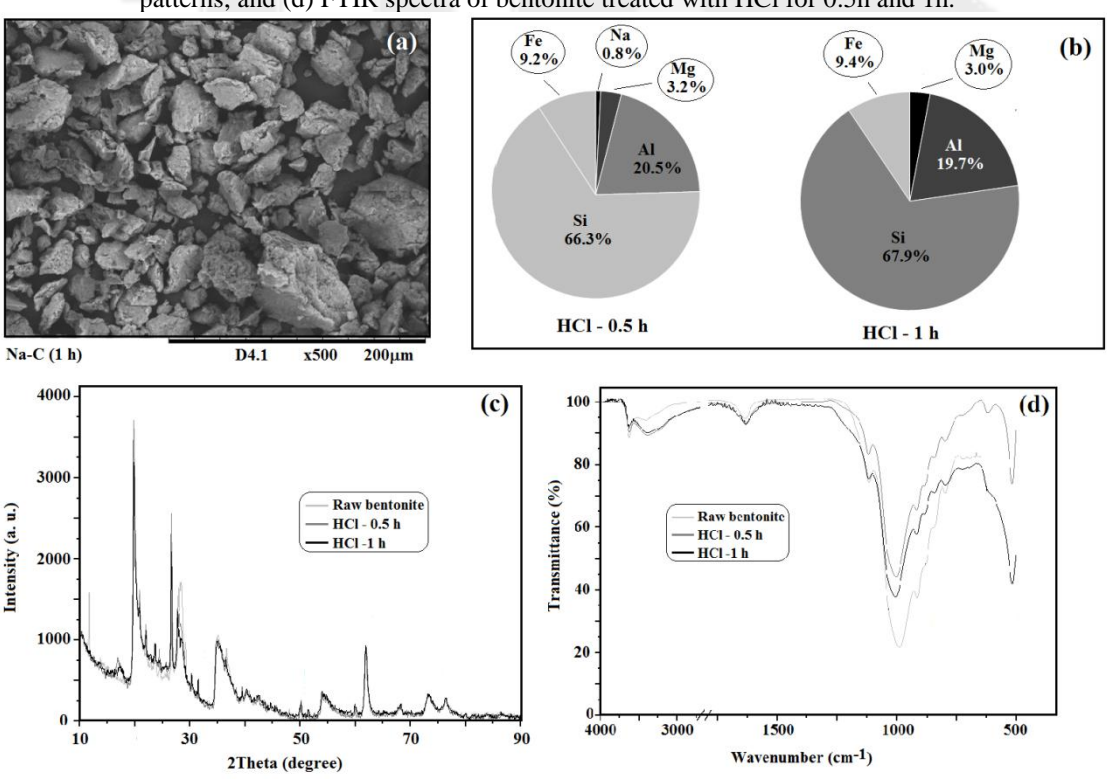
The raw bentonite (Na-35) was activated with HCl for 0.5h and 1h at 90°C. The acid activation process partially removed certain oxides, resulting in a residual composition primarily consisting of SiO₂, Al₂O₃, and Fe₂O₃. Morphological analysis revealed that the acid treatment caused particle disaggregation, yielding smaller clay particles compared to the raw bentonite (Na-35), as observed in Figure 3a and b (Alexander *et al.*, 2018).

Analysis of the X-ray diffraction patterns of the acid-treated samples (Na-C), Figure 3c, revealed a trend: as the severity of the acid treatment (i.e., treatment time) increased, the peak intensities between $2\theta = 27^{\circ}$ -29° decreased, and the peaks at $2\theta = 11.7^{\circ}$, 22.1°, and 23.7°, attributed to albite, feldspar, and halloysite (see Table 1), disappeared. This suggests that the HCl treatment affected the amounts of these minerals. The impact of acid treatment on bentonite clays varies significantly depending on the HCl concentration, treatment time, and temperature. While 1 M HCl may not significantly alter the clay structure (Elfadly *et al.*, 2017), treatment with 6 M HCl for extended periods can lead to extensive leaching and the formation of amorphous silica (Pentrák *et al.*, 2018). The acid leaching process reduces peak intensities, and the amount of amorphous material may increase with treatment severity (Askalany *et al.*, 2017).



The FTIR spectra of the acid-activated clays (Na-C) (Figure 3d) showed increased transmittance in the 3700-3300 cm⁻¹ range, attributed to v(Al(OH)Al) vibrations, compared to the raw bentonite (Na-35). This is likely due to the increased contribution of hydroxyl groups from Si-OH bonding, consistent with the compositional analysis. The acid treatment-induced leaching removed certain components, resulting in increased degrees of freedom for the remaining groups (Luna *et al.*, 2018). The sample treated with HCl for 1h exhibited lower intensity bands in the 1100-800 cm⁻¹ range, which may be related to binding modes of OH groups (Elfadly *et al.*, 2017). Given that the amounts of Al₂O₃ and Fe₂O₃ remained approximately constant before (Figure 2a) and after (Figure 3a) acid treatment (Na-C), it is likely that these oxides were not significantly dissolved, and the octahedral cations were not substantially removed ((Elfadly *et al.*, 2017).

Figure 3. HCl-treated bentonite (Na-C): (a) SEM/BSE image after 1h treatment; (b) semi-quantitative elemental composition (wt%) obtained by SEM/EDS after 0.5h and 1h treatment; (c) X-ray diffraction patterns; and (d) FTIR spectra of bentonite treated with HCl for 0.5h and 1h.



Source: Prepared by the authors themselves.



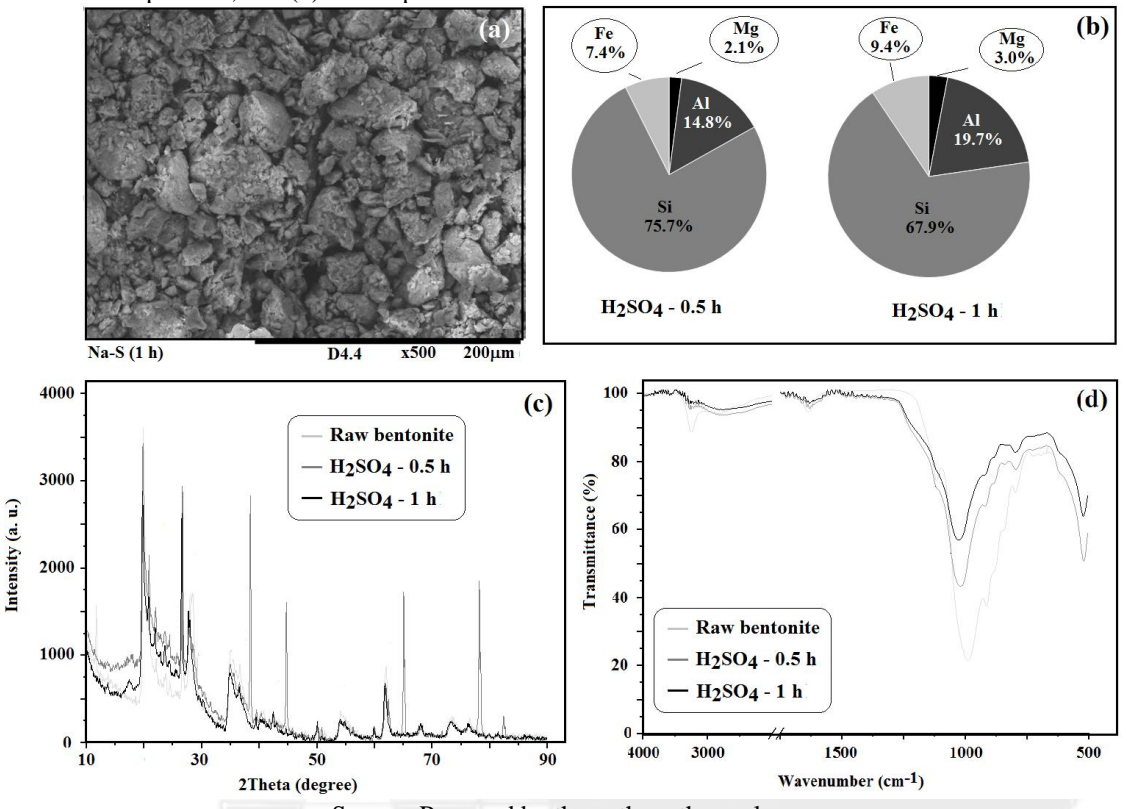
3.3 ACID TREATED BENTONITE – H₂SO₄ (N-S)

The acid treatment severity was greater for the bentonite exposed to H₂SO₄ for 0.5h compared to the 1h treatment, as evident in Figure 4b, where more pronounced removal of Fe and Al oxides was observed. The morphology of the sample treated for 1h (Figure 4a) revealed more distinct clay layers, likely due to acid leaching, which may increase the bentonite surface area (Jeenpadiphat and Tungasmita, 2014).

The XRD patterns (Figure 4c) indicated distinct phase compositions for the samples treated for 0.5h and 1h, with results comparable to those obtained with HCl treatment. Notably, the sample treated with H₂SO₄ for 0.5h exhibited a spectrum suggestive of contamination, with several peaks unrelated to the raw bentonite. In contrast, the sample treated for 1h showed reduced peak intensities and the absence of the peak at 11.7°, indicating an increase in amorphous phase content and decreased crystallinity. The H₂SO₄ treatment partially leached the bentonite clays, while also preserving the crystal structure to some extent (Önal and Sarikaya, 2007; Nwosu *et al.*, 2018)

The FTIR analysis (Figure 4d) revealed that the acid treatment led to a decrease in the intensity of the band at 3624 cm⁻¹, attributed to -OH stretching vibrations of water and AlAlOH, AlFeOH, and AlMgOH groups, suggesting partial leaching or dissolution of Al, Mg, and Fe (Mudrinic *et al.*, 2015; Elfadly *et al.*, 2017). The original band at 987 cm⁻¹, corresponding to Si-O-(Si or Al) stretching vibrations, shifted to 1026 cm⁻¹ (v(Si-O)) with reduced transmittance, indicating possible partial amorphization of the clay (Elfadly *et al.*, 2017; Silva *et al.*, 2019). The band at 794 cm⁻¹, related to v(Si-O) vibrations of kaolin and various forms of silica, particularly amorphous silica, remained at the same wavenumber but exhibited a significant decrease in intensity (Nwosu *et al.*, 2018; Koksal *et al.*, 2011).

Figure 4. H₂SO₄-treated bentonite (Na-S): (a) SEM/BSE image after 1h treatment; (b) semi-quantitative elemental composition (wt%) obtained by SEM/EDS after 0.5h and 1h treatment; (c) X-ray diffraction patterns; and (d) FTIR spectra of bentonite treated with H₂SO₄ for 0.5h and 1h.



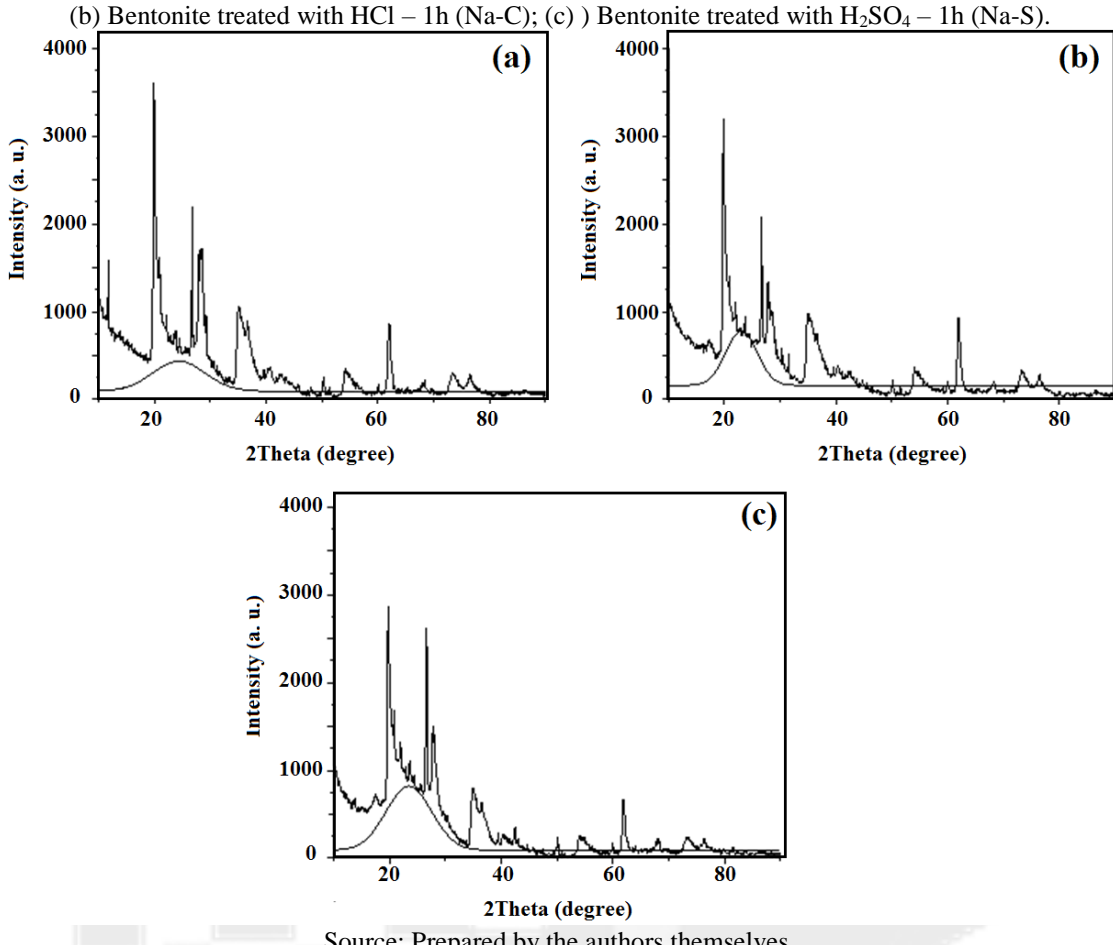
Source: Prepared by the authors themselves.

3.4 CRISTALLINITY STUDIES

Given the inconsistencies in the XRD results for samples treated with HCl or H₂SO₄ for 30 min due to contamination, the analysis focused on samples treated for 1h. Gauss fitting was applied to each diffractogram (see Figure 5) to estimate the amorphous phase content. The results indicated that H₂SO₄ was more effective in reducing the crystallinity of bentonite (Table 2) compared to HCl, likely due to its ability to remove octahedral cations (Al³⁺) and promote the formation of amorphous silica (Si-OH bonds) (Fernandes *et al.*, 2020). Nevertheless, both acids can disrupt the clay structure and lead to the formation of amorphous silica, depending on the treatment parameters (molarity, time, temperature, etc.) (Luna *et al.*, 2018).



Figure 5. X-ray diffraction patterns showing samples' degree of crystallinity: (a) Raw bentonite (Na-35);



Source: Prepared by the authors themselves.

Table 2. Samples' degree of crystallinity and amorphous Cristallinity (%) Amorphous (%) Sample Na-35 85.43 15.57 Na-C-1h84.38 15.62 71.65 28.35 Na-S-1h

Source: Prepared by the authors themselves.

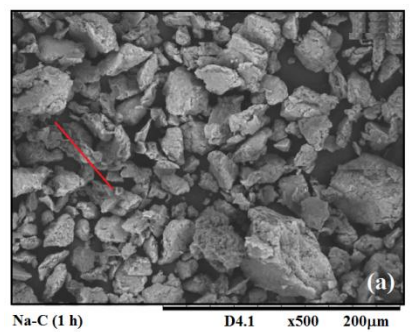
3.5 MICROSCOPY IMAGE ANALYSIS

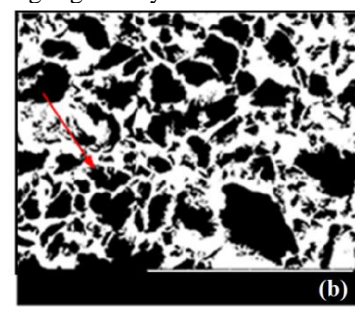
For image processing and analysis, SEM images were analyzed using ImageJ software (Ferreira and Rasband, 2012; Mathiazhagan et al., 2021). The images were segmented to identify particles as objects of interest (Figure 6). However, particle aggregates may be misinterpreted as single objects (as indicated by the red arrow in Figure 6b), leading to inaccurate particle counting. To mitigate this issue, the 'watershed' operator was applied in ImageJ (Figure 6c), which enhances object contours by detecting

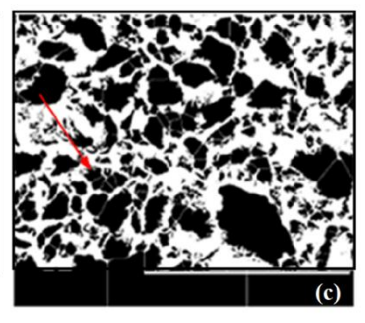


gray level discontinuities at the edges, thereby improving image segmentation (Krebbers *et al.*, 2023).

Figure 6. Image processing and analysis workflow: (a) Original SEM image of Na-C – 1h, with an aggregate highlighted by a red arrow; (b) Segmented image showing the isolated aggregate (red arrow); (c) Application of the morphological operator 'watershed' to separate individual particles, with a particle highlighted by a red arrow.







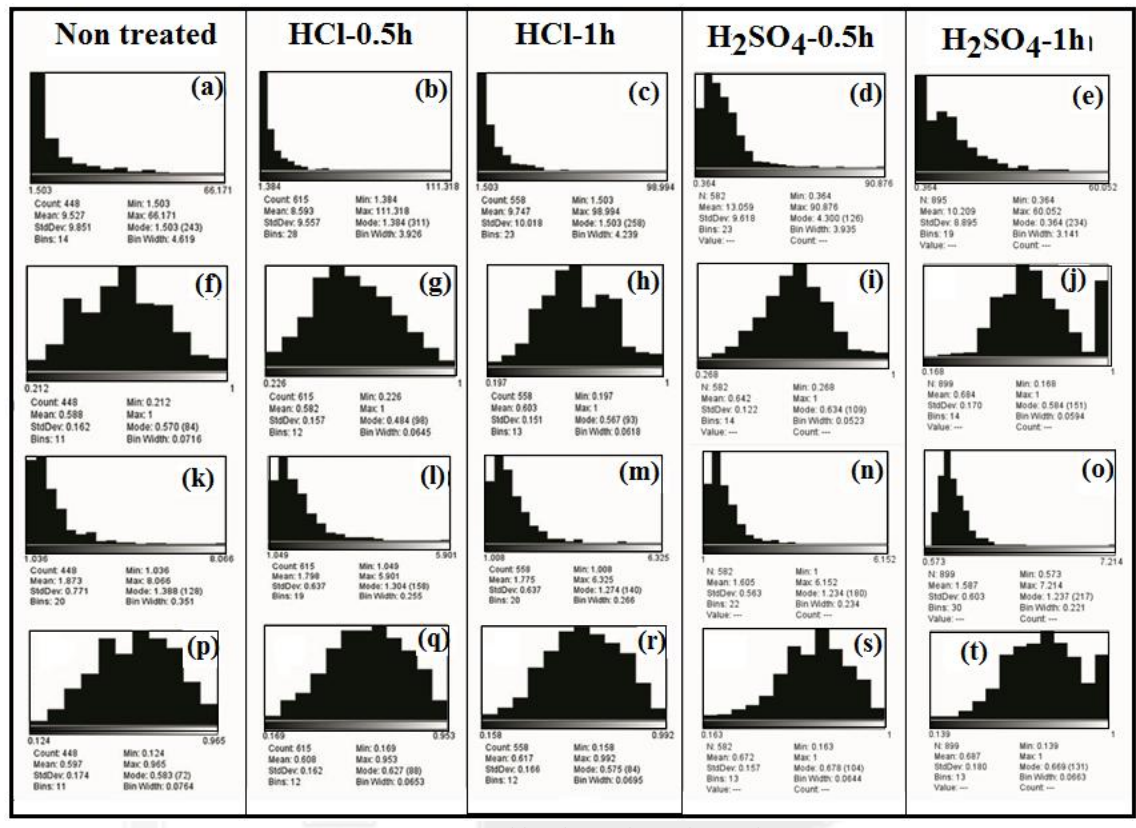
Source: Prepared by the authors themselves.

The Feret's diameter (DF) and shape parameters (circularity (C), aspect ratio (AR), and roundness (R)) were calculated (Shahin et al., 2006; Ferreira and Rasband, 2012; Santana et al., 2019; Mathiazhagan et al., 2021). The results for the untreated sample (Na-35), HCl-treated clays (Na-C), and H₂SO₄-treated clays (Na-S) can be observed and compared in Figure 7 and Table 3. Circularity values close to 1, Figure 7(d-f), indicate nearly perfect circular shapes (Ferreira and Rasband, 2012). The Aspect Ratio (AR) requires correction for particle major and minor axes, Figure 7(g-i), while Roundness (R) is the inverse of AR, Figure 7(j-1) with a maximum value of 1.00 indicating high roundness despite possible recesses (Ferreira and Rasband, 2012; Wadell, 1932). The untreated particles had a Feret diameter of 1.503 µm, similar to particles treated with HCl for 1h (1.503 µm), whereas particles treated with HCl for 0.5h had a smaller Feret diameter (1.384 μm). In contrast, H₂SO₄-treated samples had larger Feret diameters than HCl-treated samples. Notably, smaller particles (HCl-0.5h) exhibited lower adsorption capacity, potentially due to aggregation (Miyamoto et al., 2000). HCl-treated bentonite showed higher aspect ratios, indicating a more fibrous morphology, whereas H₂SO₄treated bentonite was more spherical, as confirmed by the roundness parameter. High roundness may result from extensive leaching (Cheng et al., 2018), and the high methylene blue (MB) adsorption onto H₂SO₄-activated bentonite suggests effective



activation (Bayram *et al.*, 2021). Increased aspect ratio may also indicate extensive exfoliation, leading to bentonite nanoparticles (Gao *et al.*, 2022).

Figure 7. (a-e) Samples' Feret diameter- DF; (f-j) circularity - C; (k-o) aspect ratio – RA; (p-t) roundness – R.



Source: Prepared by the authors themselves.

Table 3. Samples' Feret diameter, circularity, aspect ratio, roundness.

Samples	Na-35	Na-C	Na-C	Na-S	Na-S
		(0.5h)	(1h)	(0.5h)	(1h)
Feret diameter (µm)	9.52 ± 9.85	8.59±9.55	9.74±10.01	13.05±9.61	10.20±8.89
Circularity (µm)	0.58 ± 0.16	0.58 ± 0.15	$0.60 \pm .015$	0.64 ± 0.12	0.68 ± 0.17
Aspect ratio	1.87 ± 0.77	1.79 ± 0.63	1.77 ± 0.63	1.60 ± 0.56	1.58 ± 0.60
Roundness (µm)	0.59 ± 0.17	0.60 ± 0.16	0.61 ± 0.16	0.67 ± 0.15	0.68 ± 0.18

Source: Prepared by the authors themselves.

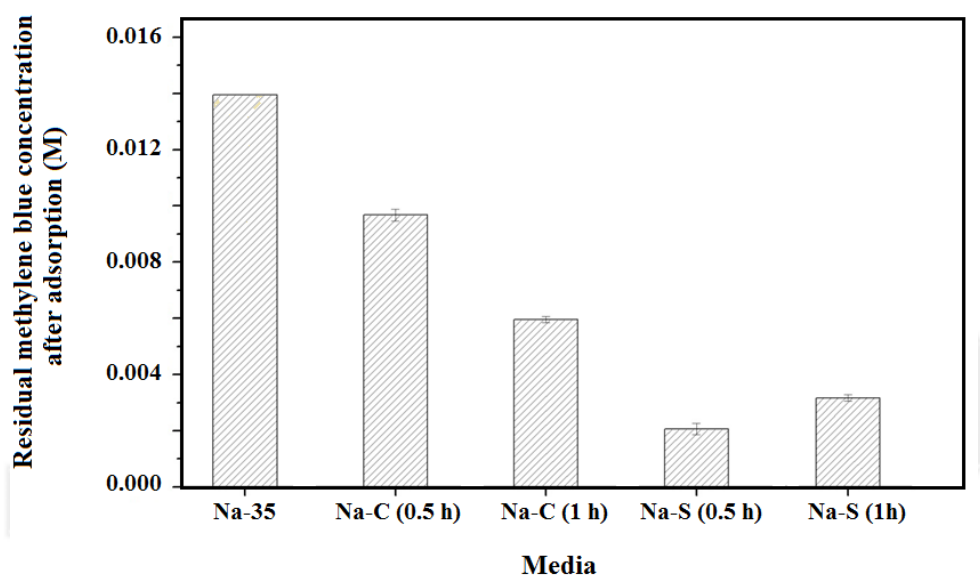
3.6 ADSORPTION OF METHYLENE BLUE (MB)

Figure 8 shows the residual methylene blue concentration onto bentonite clay samples after adsorption tests. It could be seen that, after chemical activation with hydrochloric and sulfuric acids, a significant improvement in adsorption capacity was



observed, with the NA-S (0.5 h) sample being the most effective. The chemical treatment likely increased the pore size, volume, and distribution, as well as the specific surface area of the clays (Fernandes *et al.*, 2020). Nevertheless, extending the reaction time with sulfuric acid from 30 min to 1h resulted in reduced adsorption. This decrease may be attributed to electrostatic repulsion between the cationic dye and active sites on the clay surface, as well as the reduction of active adsorption sites due to prolonged reaction time.

Figure 8. Residual methylene blue concentration onto bentonite clay samples after adsorption tests: Na-35; Na-C (0.5 and 1h) and Na-S (0.5 and 1h) demonstrating their adsorption capacity.



Source: Prepared by the authors themselves.

4 CONCLUSIONS

The bentonite clay from Novo Hamburgo/Brazil presented the characteristic oxides (SiO₂, Al₂O₃, Fe₂O₃) and exchangeable cations (Na₂O, MgO, CaO), as expect. The acid treatment with HCl does not seem to leach completely the clay, where Al₂O₃ and Fe₂O₃ were present before and after treatment. H₂SO₄ treatment seemed a more severe one, where partial leaching took place, which was confirmed by the samples' crystallinity degree after treatment. These data were confirmed by FTIR and SEM, where bands intensity varied and clays' layers were revealed by acid treatment, respectively. The UV assay demonstrated the significant influence of acid treatment parameters (type and duration) on methylene blue adsorption. Notably, chemical activation with sulfuric and





hydrochloric acids improved the adsorption of methylene blue, with the NAS-0.5 h sample exhibiting the highest adsorption efficiency.

ACKNOWLEDGEMENTS

This study was financed in part by the Coordenação de Aperfeiçoamento de Pessoal de Nível Superior - Brasil (CAPES) - Finance Code 001.





REFERENCES

ABDULLAHI, A.A. *et al.* Physicochemical analysis and heavy metals remediation of pharmaceutical industry effluent using bentonite clay modified by H₂SO₄ and HCl, **Turk. J. Chem.**, 7, 727-744, 2020. https://doi.org/10.18596/jotcsa.703913

AISHAT, A.B. *et al.* Effect of activation on clays and carbonaceous materials in vegetable oil bleaching: State of art review. **Curr. Appl. Sci. Technol.**, 5, 130-141, 2015. https://doi.org/10.9734/BJAST/2015/11942

ALEXANDER, J.A. *et al.* Simultaneous determination of cation exchange capacity and surface area of acid activated bentonite powders by methylene blue sorption. **Appl. Surf. Sci.**, 258, 2534-2539, 2012. https://doi.org/10.1016/j.apsusc.2011.10.088

ALEXANDER, J.A. *et al.* Physicochemical characteristics of surface modified Dijah-Monkin bentonite. **Particul. Sci. Technol.**, 36, 287-297, 2018. https://doi.org/10.1080/02726351.2016.1245689

ASKALANY, A.A. *et al.* High potential of employing bentonite in adsorption cooling systems driven by low grade heat source temperatures. **Energy**, 141, 782-791 (2017). https://doi.org/10.1016/j.energy.2017.07.171

BANGAR, S.P. *et al.* Bentonite clay as a nanofiller for food packaging applications. **Trends Food Sci. Technol.**, 142, 104242, 2023. https://doi.org/10.1016/j.tifs.2023.104242.

BAYRAM, H. *et al.* Optimization of bleaching power by sulfuric acid activation of bentonite. **Clay Miner.**, 56, 148-155, 2021. https://doi.org/10.1180/clm.2021.28

BELKHIR, N.L. *et al.* Manufacturing of starch nanocrystals graft polycaprolactone catalyzed by natural clay: Synthesis, characterizations, and thermal and antioxidant properties. **J. Macromol. Sci. B**, 63, 857-876, 2024. https://doi.org/10.1080/00222348.2023.2290319

BONILLA-BLANCAS, A.E. *et al.* Molecular interactions arising in polyethylene-bentonite nanocomposites. **J. Appl. Polym. Sci.**, 136, 46920, 2019. https://doi.org/10.1002/app.46920

BORAH, D. *et al.* Modification of bentonite clay & its applications: A review. **Rev. Inorg. Chem.**, 42, 265-282, 2022. https://doi.org/10.1515/revic-2021-0030

CAGLAR, B. *et al.* Characterization of Unye bentonite after treatment with sulfuric acid. **Quím. Nova**, 36, 955-959, 2013. https://doi.org/10.1590/S0100-40422013000700006.

CARMO, A.L.V. *et al.* Ageing characteristics related to cation exchange and interlayer spacing of some Brazilian bentonites. **Heliyon**, 7, e06192, 2021. https://doi.org/10.1016/j.heliyon.2021.e06192





CHAARI, I. *et al.* Comparative study on adsorption of cationic and anionic dyes by smectite rich natural clays. **J. Mol. Struct.**, 1179, 672-677, 2019. https://doi.org/10.1016/j.molstruc.2018.11.039

CHENG, Y. *et al.* Surface textural analysis of quartz grains from modern point bar deposits in lower reaches of the yellow river. **IOP Conf. Ser.: Earth Environ. Sci.**, 108, 032023, 2018. https://doi.org/10.1088/1755-1315/108/3/032023

COUTO JUNIOR, O.M. *et al.* Study on coagulation and flocculation for treating effluents of textile industry. **Acta Sci. Technol.**, 35, 83-88, 2013. https://doi.org/10.4025/actascitechnol.v35i1.11685

DEHGHANI, M.H. *et al.* Removal of methylene blue dye from aqueous solutions by a new chitosan/zeolite composite from shrimp waste: Kinetic and equilibrium study. **Korean J. Chem. Eng.,** 34, 1699-1707, 2017. https://doi.org/10.1007/s11814-017-0077-2

De LEÓN, A.T. *et al.* Adsorption of Cu ions onto a 1.10 phenanthroline-grafted Brazilian bentonite. **Clays Clay Miner.**, 51, 58-64, 2003. https://doi.org/10.1346/CCMN.2003.510107

DÍAZ, F.R.V.; SANTOS, P.S. Studies on the acid activation of Brazilian smectitic clays. **Quim. Nova**, 24, 345-353, 2001. https://doi.org/10.1590/S0100-40422001000300011

DIMBO, D. *et al.* Methylene blue adsorption from aqueous solution using activated carbon of spathodea campanulata. **Results Eng.**, 21, 101910, 2024. https://doi.org/10.1016/j.rineng.2024.101910

ELFADLY, A.M. *et al.* Production of aromatic hydrocarbons from catalytic pyrolysis of lignin over acid-activated bentonite clay. **Fuel Process. Technol.**, 163, 1-7, 2017. https://doi.org/10.1016/j.fuproc.2017.03.033

FAJARDO, T.V.M. *et al.* High-throughput sequencing applied for the identification of viruses infecting grapevines in Brazil and genetic variability analysis. **Trop. Plant. Patho.**, 42, 250-260, 2017. https://doi.org/10.1007/s40858-017-0142-8

FERNANDES, J.V. *et al.* Adsorption of anionic dye on the acid-functionalized bentonite. **Mater.**, 13, 3600, 2020. https://doi.org/10.3390/ma13163600

FERREIRA, T.; RASBAND, W. ImageJ User Guide-IJ1.46r ImageJ, 1-91, 2012. http://imagej.nih.gov/ij/docs/guide

GANDHI, D. *et al.* Naturally occurring bentonite clay: Structural augmentation, characterization and application as catalyst. **Mater. Today Proc.**, 57, 194-201, 2022. https://doi.org/10.1016/j.matpr.2022.02.346





GAO, Y. *et al.* Preparation of montmorillonite nanosheets with a high aspect ratio through heating/rehydrating and gas-pushing exfoliation. **Langmuir**, 38, 10520, 2022. https://doi.org/10.1021/acs.langmuir.2c01320

GONZÁLEZ-SANTAMARÍA, D.E. *et al.* SEM-EDX study of bentonite alteration under the influence of cement alkaline solutions. **Appl. Clay Sci.**, 212, 106223, 2021. https://doi.org/10.1016/j.clay.2021.106223

HAMAD, H.N. *et al.* Optimized bentonite clay adsorbents for methylene blue removal. **Processes**, 12, 738, 2024. https://doi.org/10.3390/pr12040738

JEENPADIPHAT, S.; TUNGASMITA, D.N. Esterification of oleic acid and high acid content palm oil over an acid-activated bentonite catalyst. **Appl. Clay Sci.**, 87, 272-277, 2014. https://doi.org/10.1016/j.clay.2013.11.025

KOKSAL, E. *et al.* Structural characterization of aniline-bentonite composite by FTIR, DTA/TG, and PXRD analyses and BET measurement. **Spectrosc. Lett.**, 44, 77-82, 2011. https://doi.org/10.1080/00387010903555953

KREBBERS, L.T. *et al.* Computed tomography of flake graphite ore: Data acquisi-tion and image processing. **Miner.**, 13, 247, 2023. https://doi.org/10.3390/min13020247

LEODOPOULOS, C. *et al.* Adsorption of cationic dyes onto bentonite. **Sep. Purif. Rev.**, 44, 74-107, 2015. https://doi.org/10.1080/15422119.2013.823622

LIMA, E.M.B. *et al.* Poly(lactic acid) biocomposites with mango waste and organomontmorillonite for packaging. **J. Appl. Polym. Sci.**, 136, 47512, 2019. https://doi.org/10.1002/app.47512

LUNA, F. *et al.* Natural and modified montmorillonite clays as catalysts for synthesis of biolubricants. **Mater.**, 11, 1764, 2018. https://doi.org/10.3390/ma11091764

MANO, E.S. *et al.* Mineralogical characterization of Ni-bearing smectites from Niquelândia, Brazil. **Clays and Clay Miner.**, 62, 324-335, 2014. https://doi.org/10.1346/CCMN.2014.0620406

MATHIAZHAGAN, S. *et al.* Ecofriendly antimicrobial Acalypha indica leaf extract immobilized polycaprolactone nanofibrous mat for food package applications. **J. Food Process. Preserv.**, 45, e15302, 2021. https://doi.org/10.1111/jfpp.15302

MIYAMOTO, N. *et al.* Adsorption and aggregation of a cationic cyanine dye on layered clay minerals. **Appl. Clay Sci.**, 16, 161-170, 2000. https://doi.org/10.1016/S0169-1317(99)00051-4

MORAES, D.S. *et al.* Mineralogy and chemistry of a new bentonite occurrence in the eastern Amazon region, northern Brazil. **Appl. Clay Sci.**, 48, 475-480, 2010. https://doi.org/10.1016/j.clay.2010.02.009





MUDRINIĆ, T. *et al.* Electrochemical activity of iron in acid treated bentonite and influence of added nickel. **Appl. Surf. Sci.**, 353, 1037-1045, 2015. https://doi.org/10.1016/j.apsusc.2015.07.054

NWOSU, F.O. *et al.* Reparation and characterization of adsorbents derived from bentonite and kaolin clays. **Appl. Water Sci.**, 8, 195, 2018. https://doi.org/10.1007/s13201-018-0827-2

ÖNAL, M.; SARIKAYA, Y. Preparation and characterization of acid-activated bentonite powders. **Powder Technol.**, 172, 14-18, 2007. https://doi.org/10.1016/j.powtec.2006.10.034

PENTRÁK, M. *et al.* Alteration of fine fraction of bentonite from Kopernica (Slovakia) under acid treatment: A combined XRD, FTIR, MAS NMR and AES study. **Appl. Clay Sci.**, 163, 204-213, 2018. https://doi.org/10.1016/j.clay.2018.07.028

PIMRAKSA, K. *et al.* Geopolymer/zeolite composite materials with adsorptive and photocatalytic properties for dye removal. **Plos One**, 15, e0241603, 2020. https://doi.org/10.1371/journal.pone.0241603

RIGO, M.L. *et al.* The residual shear strength of tropical soils. **Can. Geotech. J.**, 43, 431-447, 2006. https://doi.org/10.1139/t06-015

SANTANA, G.L. *et al.* A comparative study of particle size distribution using analysis of variance for sedimentation and laser diffraction methods. **Cerâmica**, 65, 452-460, 2019. https://doi.org/10.1590/0366-69132019653752623

SANTOS, D.C. *et al.* Application of carbon composite adsorbents prepared from coffee waste and clay for the removal of reactive dyes from aqueous solutions. **J. Braz. Chem. Soc.**, 26, 924-938, 2015. https://doi.org/10.5935/0103-5053.20150053

SHAHIN, M.A. *et al.* Determining soya bean seed size uniformity with image analysis. **Biosyst. Eng.**, 94, 191-198, 2006. https://doi.org/10.1016/j.biosystemseng.2006.02.011

SILVA, A.S. *et al.* Wet peroxide oxidation of paracetamol using acid activated and Fe/co-pillared clay catalysts prepared from natural clays. **Catalysts**, 9, 705, 2019. https://doi.org/10.3390/catal9090705

SOARES, B.G. *et al.* Modification of anionic and cationic clays by zwitterionic imidazolium ionic liquid and their effect on the epoxy-based nanocomposites. **Appl. Clay Sci.**, 135, 347-354, 2017. https://doi.org/10.1016/j.clay.2016.10.016

SU, H. *et al.* Optimization of decoloring conditions of crude fatty acids recovered from crude glycerol by acid-activated clay using response surface method. **Korean J. Chem. Eng.**, 31, 2070-2076, 2014. https://doi.org/10.1007/s11814-014-0158-4





ULAKPA, W. C. et al. Statistical optimization of biodiesel synthesis from waste cooking oil using NaOH/bentonite impregnated catalyst. Cleaner Waste Systems, 3, 100049, 2022. https://doi.org/10.1016/j.clwas.2022.100049

ULLAH, Z. et al. Use of HCl-modified bentonite clay for the adsorption of Acid Blue 129 from aqueous solutions. **Desalin. Water Treat.**, 57, 8894-8903 (2016). https://doi.org/10.1080/19443994.2015.1027282

WADELL, H. Volume, Shape, and Roundness of Rock Particles. J. Geol., 40, 443-451, 1932. https://www.jstor.org/stable/30058012

ZHIRONG, L. et al. FT-IR and XRD analysis of natural Na-bentonite and Cu(II)-loaded Na-bentonite. Spectrochim. Acta A Mol. Biomol. Spectrosc., 79, 1013-1016, 2011. https://doi.org/10.1016/j.saa.2011.04.013

